PREDICTION OF DELAMINATION

IN BRAIDED COMPOSITE T-PIECE SPECIMENS

Jiye Chen, Eric Ravey**, Stephen Hallett***,*

*Michael Wisnom*** and Marcello Grassi *****

**University of Portsmouth, Portsmouth PO1 3AH, UK*

***Rolls-Royce Ltd, Derby DE24 8BJ, UK*

****University of Bristol, Bristol BS8 1TR, UK*

*****QinetiQ, Farnborough, Hants GU14 0LX, UK*

Keywords: A. Polymer-matrix composites (PMCs); B. Modelling; C. Delamination; E. Braiding; T-piece cohesive models

Abstract:

This paper presents an approach to predict the delamination of braided composite T-piece specimen using cohesive models. As part of an investigation on simulation of delamination in T-piece specimens, cohesive elements from ABAQUS were employed in forming a cohesive model to study the progressive delamination. Predictions given by the model of single delamination together with experimental results are presented. These results suggest that prediction of progressive delamination using cohesive models is feasible. Finally this paper proposes future work for precise prediction of delamination of braided composite T-piece specimens.

1. Introduction

T-piece specimens have been paid a high degree of attention in the study of behavior of aerospace composite structures because they are representative of features in key aerospace structures such as composite vanes in aero engines and T and I stiffeners and beams such as stringers [1, 2]. Study of the failure mechanisms in T-piece specimens and prediction of their damage resistant capability is fundamental for the design of such composite components. This paper aims to investigate the failure of T-piece specimens by simulating delamination propagation under a mechanical "pull-off" load case.

The T-piece specimen investigated in this publication is a carbon fibre based braided composite specimen, which consists of a vertical blade, radius transition region, a horizontal base and a uniform unidirectional deltoid also called gap filler. Experimental test work at quasi-static strain rates was investigated [3]. This showed the main failure mode to be delamination. Figure 1 shows the local delamination pattern in the area of the deltoid of one failed specimen. The failure mode is multiple delaminations progressing from the point of initiation. The dominant delamination is along the interface between the deltoid and braid ply in the radius area. This starts at the location of higher interlaminar stresses which is in the upper half of the curved interface in the radius region as indicated in Figures 1 and 4. This location is recognised as the initial failure point. From this location delamination not only grows down along the curved interface but also grows up to the end of laminate blade. It should be noted that the test failure loads given refer to initial failure loads and ultimate failure loads [3]. These values relate to the point of initiation and the point of maximum load, once delamination has propagated significantly.

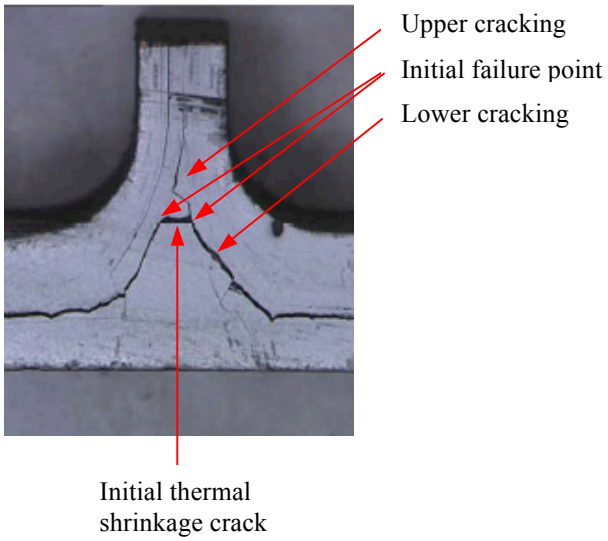

Fig. 1 Failure modes of T-piece specimen

Delamination crossing through deltoid can also be seen in Figure 1. This is considered to be due to thermal effects from the curing process.

This paper presents the numerical simulation of progressive delamination, the main failure mode of the T-piece specimens, using finite element cohesive interface models. This modelling work focuses on the simulation of a single dominant delamination between the deltoid and braid ply in the radius area, which develops down to the base from the initial failure point. This work aims to determine the failure load at this single delamination by simulation.

2. Geometry, materials properties and loading

Figure 2 shows the 2D finite element model with the definition of geometry of T-piece specimens, boundary conditions.

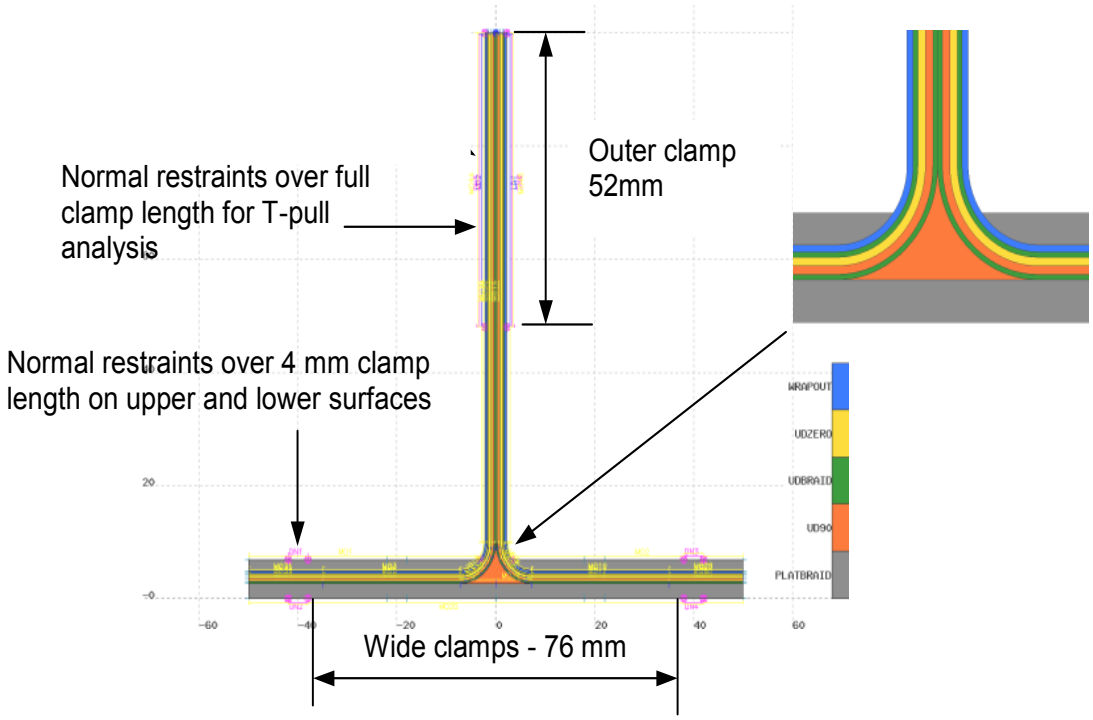

Fig. 2 A 2D finite element model

Figure 3 shows the deflected shape of the T-Piece specimen under the pulling force which defines the loading case considered in this study.

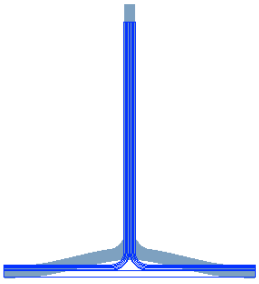

Fig. 3 T-Piece under pulling force

The width of specimen is 20mm, the thickness of the upper arm is 4.4mm and the total thickness of the base is 6.87mm. The material is a braided carbon fibre composite. A schematic configuration of the laminates can be seen in Figure 2 with details of lay-up. Material properties of each layer are given in Table 1.

Table 1 Materials properties

	E_{11} (GPa)	E_{22} (GPa)	E_{33} (GPa)	G_{12} (GPa)	G_{13} (GPa)	G_{23} (GPa)	ν12	ν13	ν23
Outer Braided Wrap	59.7	60.1	9.7	21.95	4.7	4.7	0.279	0.28	0.28
Braided UD layer	160	9.7	9.7	5.9	5.9	4.7	0.33	0.33	0.28
[0°] layer	152	9.7	9.7	5.9	5.9	4.7	0.33	0.33	0.28
[90°] layer and Deltoid	9.7	152.0	9.7	5.9	4.7	5.9	0.021	0.28	0.33
Platform Braids	65.8	46.1	9.7	25.8	4.7	4.7	0.421	0.28	0.28

It should be noted that so far there are no reported fundamental fracture tests for such material. The fracture energy and interlaminar material strength given in Table 2 are trial ones based on literature for other composites [4, 5, 6, 7]. This affects the accuracy of comparison between modelling prediction and test results since only approximate values were assumed. For this reason the investigation of effects of varying fracture energy by ± 50% and varying interlaminar material strength by ±50% on prediction are given in this paper.

Table 2 Interlaminar material strength and fracture energy

σ33c (MPa)	σ13c (MPa)	σ23c (MPa)	G_{Ic} J/m^2	G_{IIc} J/m^2	G_{IIIc} J/m^2
45	35	35	300	1000	1000

3. Modelling Delamination

A half plane strain model has been set up due to its symmetric features, as shown in Figure 4.

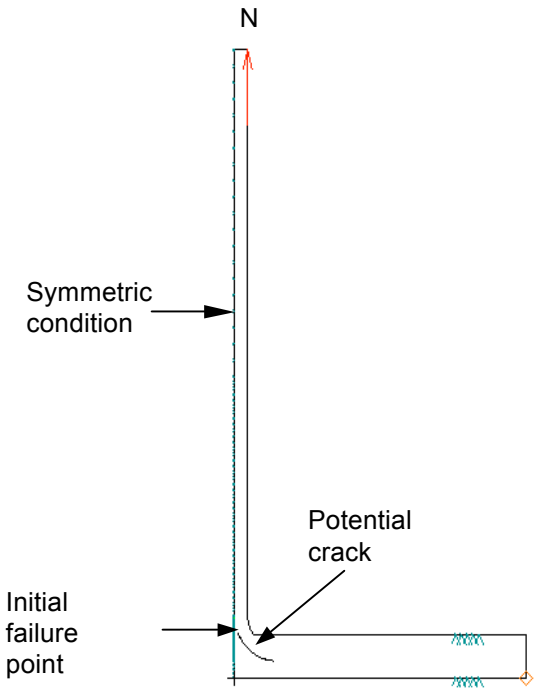

Fig. 4 Half 2D model definition

It should be noted that the initial failure point indicated in Figure 4 was determined by considering failed test samples shown in Figure 1 and interlaminar stresses supplied by a static stress analysis [8].

The potential crack path shown in Figure 5 was determined from experimental observations such as in Figure 1, which shows the most dominant delamination. Figure 5 also shows a local mesh of the radius and deltoid regions. The interface between the laminate radius and deltoid is the potential cracking path into which cohesive interface elements were inserted.

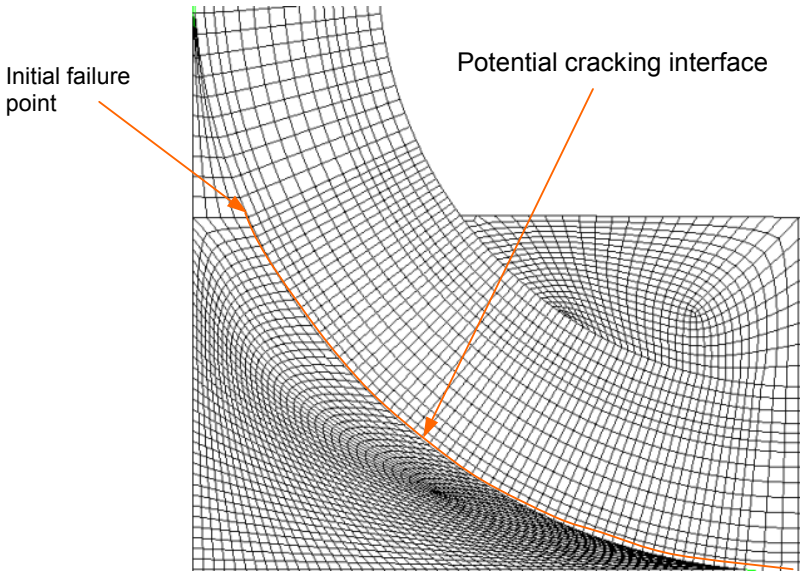

Fig. 5 The mesh around cracking interface

Basic plane strain elements CPE4 and 2-D cohesive elements COH2D4 from ABAQUS were employed in this investigation [9]. Plane strain elements were used for the plies and the deltoid of T-piece. Cohesive elements were applied along the potential cracking interface. The critical crack length a_m is about 0.36mm as calculated from the linear fracture mechanics based formula in Eq. 1.

$$a_m = \frac{G_c E}{\psi^2 \sigma_c^2 \pi} \qquad (1)$$

where, fracture energy G_c is taken as G_{Ic}, material property E is taken as E_{33} of UD ply and interlaminar strength σ_c is taken as σ_{33c}. ψ is cracking shape parameter [10] and was taken to be 1.12 in this model. The actual modelled crack length should be less than this value, and 0.125mm was therefore used as element length along potential crack path in this model, which determines the length of each cohesive element and hence ensures

that modelling of the crack can be captured below its critical length. It should be noted however that no pre-crack was inserted. This analysis has been run using ABAQUS/standard code with displacement control. From the initial failure point delamination developed down to the bottom of deltoid. This process occurs relatively quickly.

It should be noted that a sliding restraint at the clamp position was applied in this model to consider any possible slight moving at clamp position.

4. Formulations of cohesive elements in ABAQUS

Cohesive elements can simulate several types of behaviours at interfaces when the interface load carrying capability is lost. They have been the subject of significant investigation in the open literature and are becoming widely used for the prediction of composites delamination failure [4, 6, 7,11,12]. A review by Hallett [13] describes more fully many of the different formulations that have been investigated and their applications to composite materials and structures.

Application of cohesive elements in this simulation of delamination is the key issue. Firstly, the relative displacement at damage initiation ε_c needs to be defined, which can be determined by Eq. 2.

$$\varepsilon_c = \frac{\sigma_c}{k} \qquad (2)$$

Where, σ_c and k is interlaminar strength and initial stiffness respectively for each single crack mode. The damage initiation can be accounted by the quadratic formula of Eq. 3.

$$\left(\frac{\sigma_I}{\sigma_{IC}}\right)^2 + \left(\frac{\sigma_{II}}{\sigma_{IIC}}\right)^2 + \left(\frac{\sigma_{III}}{\sigma_{IIIC}}\right)^2 = 1 \qquad (3)$$

The linear softening damage law as shown in Figure 6 [9] was employed in this model.

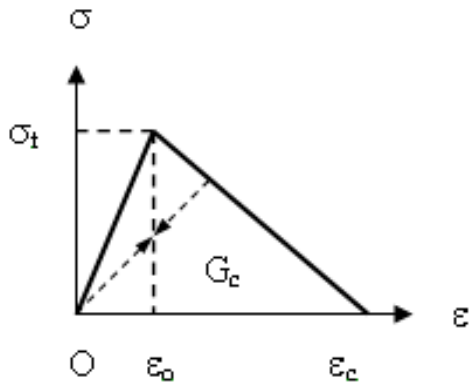

Fig. 6 Linear softening damage law

This linear softening law was used together with the mixed mode fracture energy criteria based on Benzeggagh-Kenane (BK) [14] law (Eq. 4) or the power law (Eq.5).

$$G_I^c + \left(G_{II}^c - G_I^c\right)\left(\frac{G_S}{G_T}\right)^{\alpha} = G^c \qquad (4)$$

Where, G^c is the total mixed-mode fracture energy, G_I is the normal strain energy release rate, G_{II} and G_{III} are shear strain energy release rates in two directions respectively, $G_S=G_{II}+G_{III}$. G_I^c is the normal fracture energy, G_{II}^c is shear fracture energy, the total strain energy release rate $G_T=G_I+G_S$. Equation (4) is suitable for the case when $G_{II}^c = G_{III}^c$, the mode III fracture energy.

$$\left(\frac{G_I}{G_I^c}\right)^{\alpha} + \left(\frac{G_{II}}{G_{II}^c}\right)^{\alpha} + \left(\frac{G_{III}}{G_{III}^c}\right)^{\alpha} = 1 \qquad (5)$$

The cohesive elements with zero-thickness are usually chosen for simulation of interfacial delamination in composites. These elements require the coordinates of the

node pairs on the cracking path to be checked when it is a curved interface. All nominally coincident nodes with a small difference in position (10^{-5}) in the T-piece fillet have to be corrected to be exactly coincident.

The viscosity parameter is required to be defined for stability in solving the nonlinear equations. As this slightly affects the CPU time but not the results, values from 10^{-3} to 10^{-5} were recommended and an optimum value of 10^{-4} was chosen in this model. It is noted that it would be difficult to achieve the nonlinear iteration convergence without this parameter.

5. Results using the power and BK failure criteria

All predictions in this section were obtained using the linear softening damage law plus BK energy criteria where α=1 or 2, and power law where α=1 or 2. The local deformation after delamination is shown in Figure 7, which shows the delamination is mixed mode I and mode II cracking. Figure 8 gives predicted failure loads together with experimental results, where it can be seen that there is an overall good agreement between prediction and the tested ultimate failure results.

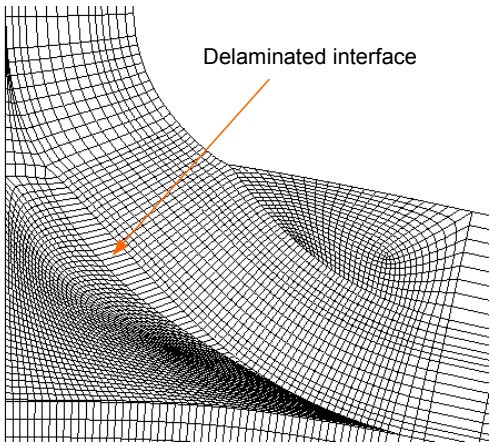

Fig. 7 Deformation after delamination

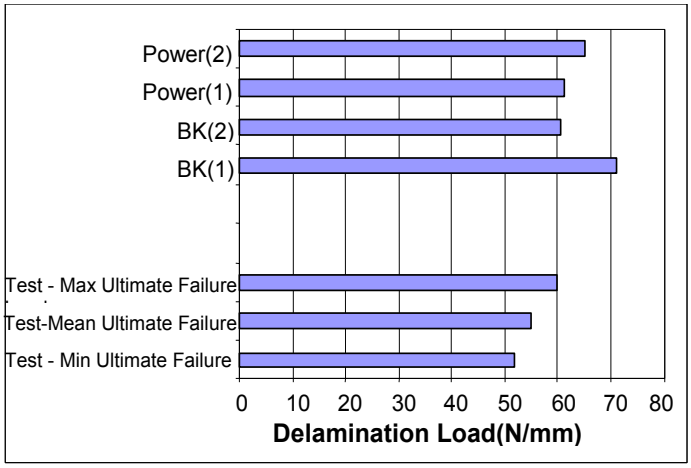

Fig. 8 Comparison between prediction and tests

Figure 9 shows the effects of different energy based failure criteria laws on the predicted load-displacement curves. When using BK(2), the predicted failure load reduced by 16% compared to BK(1), and was very close to the maximum ultimate test failure load. When using power law, the predicted failure load from the case $\alpha=1$ is 8% lower than that from the case $\alpha=2$, also very close to the maximum ultimate test failure load. Unlike the BK criteria the first order power law predicted better failure load then the second order power law. This implies that the linear power law presents a better fracture energy relationship in this mixed mode delamination case, and supplies a simple calculation in determination of delamination propagation. A similar case that a higher order power law predicts higher failure loads for mixed mode delamination was discussed in reference 6 . It should be noted that all these investigations used the fracture properties and interlaminar material strengths given in Table 2.

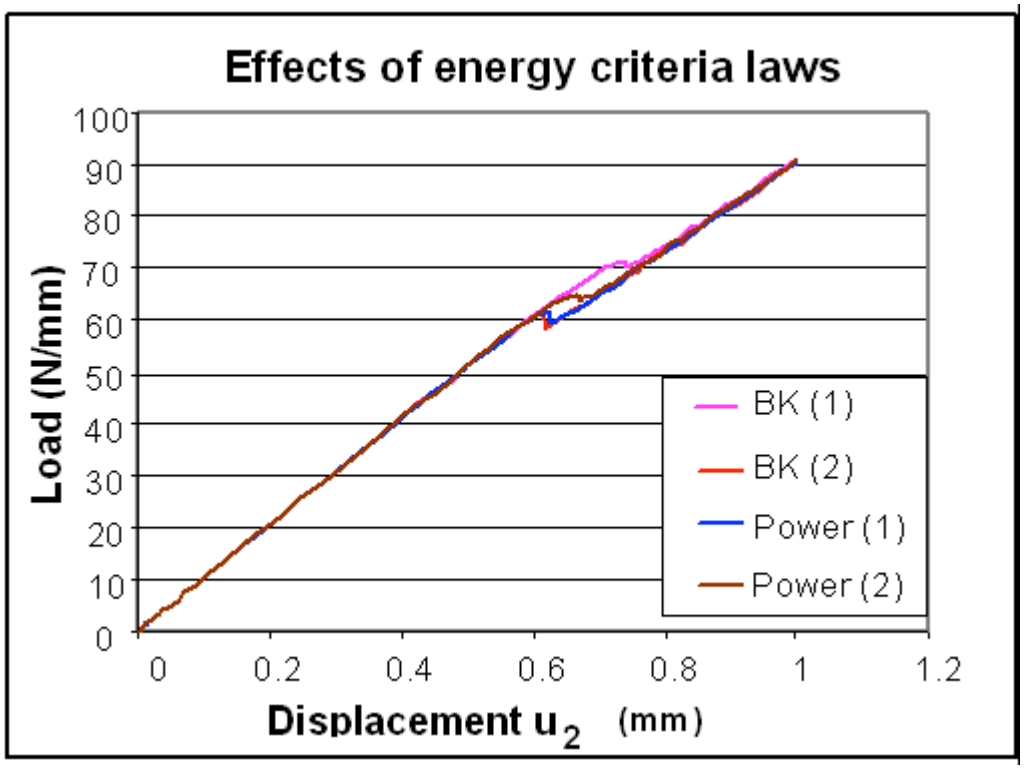

Fig. 9 Failure response with different energy criteria laws

Assuming materials data in Table 2 as the most representative fracture properties and interlaminar material strengths, the modelling prediction using the linear softening damage law plus energy criteria power law (α=1) and BK law (α = 2) with approximated fracture energy data adequately agrees with the tested ultimate failure load.

6. Investigation of effects of varying fracture properties on prediction

Because the fracture energies given in Table 2 are trial ones, it is necessary to investigate the effects of varying fracture energy on the failure prediction. Figure 10 shows such effects by giving predicted-to-mean test failure load ratios together with tested ultimate failure loads, where original materials given in Table 2 is considered to produce the mean prediction, increasing and decreasing by 50% fracture energy are referred to produce the maximum and minimum prediction respectively. Both G_{Ic} and

G_{IIc} affect the prediction in this mixed mode delamination, with G_{IIc} having a slightly greater effect than G_{Ic}.

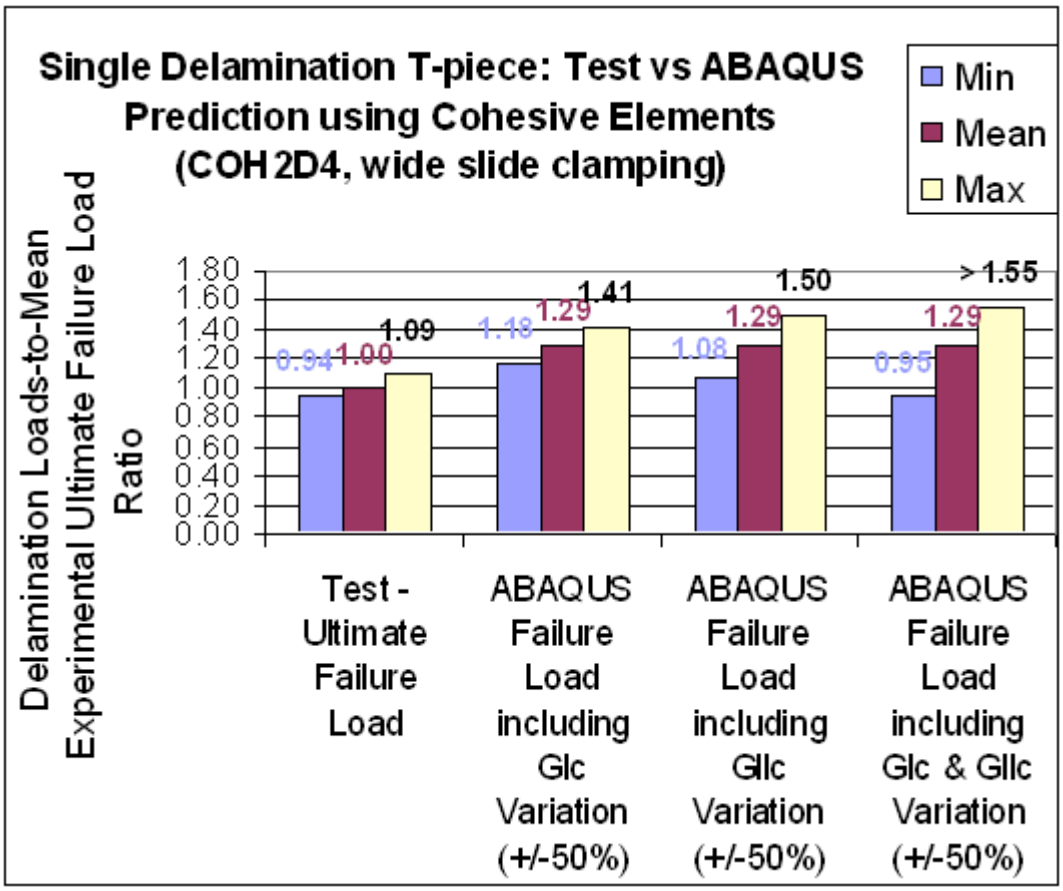

Fig. 10 Predicted-to-mean test failure load ratios for ABAQUS cohesive model with BK(α= 1)

An investigation of the effects of varying the interlaminar strength (normal strength σ_{33c} and shear strength σ_{13c}) by ±50% can be seen respectively in Figure 11 and Figure 12.

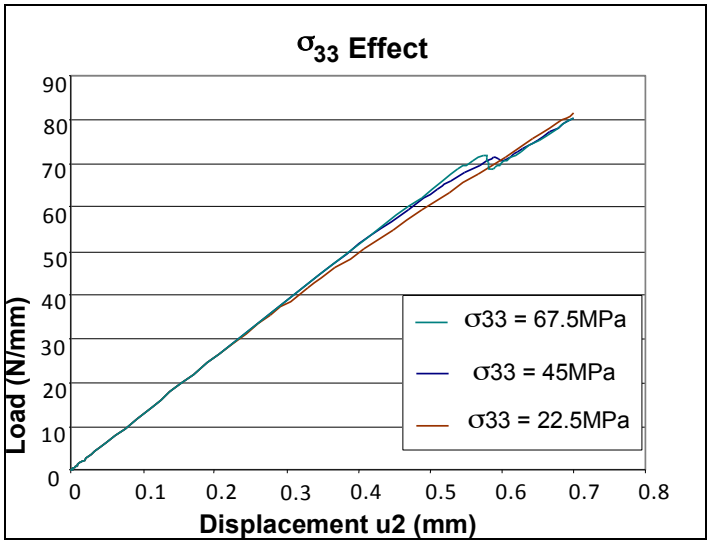

Fig. 11 Failure response with varied σ_{33}, linear softening law + BK(α=1)

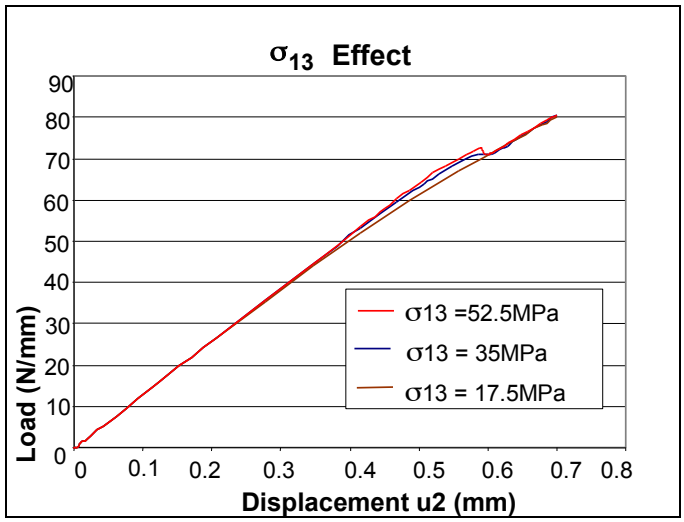

Fig. 12 Failure response with varied σ_{13}, linear softening law + BK(α=1)

Increase of interlaminar strength by 50% slightly changes the global model stiffness, but the increase in failure load is less than 5%. In addition, a reduction of interlaminar strength by 50% also slightly changes the global model stiffness, and the apparent failure point (the drop in the load-displacement curve) is lost.

7. Comments and Future work

This paper investigated the failure prediction of T-piece specimens by simulating a single delamination. It shows generally the possibility of predicting failure loads using cohesive models.

The modelling prediction using the linear softening damage law plus energy criteria power law (α=1) and Benzeggagh-Kenane law (α=2), normal fracture properties and the sliding clamp condition adequately agrees to the tested ultimate failure load without any variations of the fracture energy data. It should however be noted that these were only approximated from literature values and were not measured for the current material. The effects of varying fracture energy and interlaminar strength on prediction therefore were given as reference. This would indicate that the failure is dominated by the propagation of the crack rather than its initiation. This is consistent with many results from literature that have given rise to strategies such as that proposed by Turon et al [15] for artificially reducing the initiation stress used for interface elements to allow use of a coarser mesh. The variation in results with choice of mixed mode failure criterion used indicates the need for careful consideration in this area.

Referring to the deformed shape in Figure 7, the initial failure point appears over restrained. This means delamination would quite possibly grow up to the end of laminate blade as well as down to the base. This can be investigated by creating a model with multiple delamination sites to study their effects on failure prediction [16]

The following is suggested in future work in order to be able to achieve precise prediction:

a. fracture tests to obtain G_{Ic} and G_{IIc}.

b. analysis with thermal effects on failure prediction.

c. simulation of multiple delamination (cracks which can potentially propagate up, down and across the deltoid from the initial failure point).

8. Acknowledgements

The authors would like to acknowledge the MoD for their support of this programme. The authors would also like to acknowledge the MoD, Rolls-Royce and QinetiQ for their permission to publish.

References

1 Stickler P. B. and Ramulu M., Experimental study of composite T-joints under tensile and shear loading, Adv. Composite Mater. 2006, Vol. 15, No. 2, pp. 193–210

2 Davies GAO, Hitchings D, Ankersen J, Predicting delamination and debonding in modern aerospace composite structures, Composites Science and Technology 2006, 66 (6) pp: 846-854

3 Grassi M. and Meeks C., Structural evaluation of composite vane root T-specimens: HCF interim test summary, QinetiQ report, December 2004

4 Chen J. and New A. Application of decohesive model with mixed damage scale in fracture analysis of composite materials, International Journal of Fatigue & Fracture of Engineering Materials & Structures, 24(11), p761-769, 2001

5 Cui W, Wisnom MR. A combined stress-based and fracture-mechanics-based model for predicting delamination in composites. Composites 1993; 24:467-474

6 Chen J, Crisfield MA, Kinloch AJ, Busso EP, Matthews FL, Qiu Y. Predicting progressive delamination of composite material specimens via interface elements. Mechanics of Composite Materials and Structures 1999; 6:301-317

7 Tvergaard V, Hutchinson JW. The relation between crack growth resistance and fracture progress parameters in elastic-plastic solids. Journal of the Mechanics and Physics of Solids 1992; 40(6): 1377-1397

8 Bishop A J, A report of 2D modelling: T-Pull Analysis of Composite T-piece, Rolls-Royce internal report, June 2004

9 ABAQUS User Manual, Hibbitt, Karlsson & Sorensen Inc., 1080 Main Street, Pawtucket, RI02860-4847, USA

10 Benham P P, Crawford R J and Armstrong C G, Mechanics of engineering materials, Pearson Education, 1987

11 Goyal VK, Johnson ER, and Davila CG., Irrevesible constitutive law for modeling the delamination process using interface surface discontinuities, Composite Structures, 65, p289-305, 2004

12 Camanho PP, Davila CG, De Moura MF. Numerical simulation of mixed-mode progressive delamination in composite materials. J Composite Materials 2003;37:1415–24

13 Hallett SR, Predicting progressive delamination via interface elements, in Delamination behaviour of composites, S. Sridharan, Editor. Woodhead. 2008

14 Benzeggagh ML and Kenane M, Measurement of Mixed-Mode Delamination Fracture Toughness of Unidirectional Glass/Epoxy Composites with Mixed-Mode Bending Apparatus, Composites Science and Technology, 56, pp. 439–449, 1996.

15 Turon A, Davila CG, Camanho PP, Costa J. An engineering solution for mesh size effects in the simulation of delamination using cohesive zone models.Eng Fract Mech 2007;74:1665–82

16 Ravey EP, Investigation of composite damage tolerance and fracture assessment: delamination prediction in T-piece, Rolls-Royce internal report, June 2006